Published in final edited form as:
Mol Cancer Ther. 2012 September ; 11(9): 1884–1893. doi:10.1158/1535-7163.MCT-11-1041-T.

Killing of Kras mutant colon cancer cells via Rac-independent actin remodeling by the βGBP cytokine a physiological PI3K inhibitor therapeutically effective in vivo

Livio Mallucci[1], **Dong-yun Shi**[1,*], **Derek Davies**[2], **Peter Jordan**[2], **Alastair Nicol**[2], **Lavinia Lotti**[3], **Renato Mariani-Costantini**[4], **Fabio Verginelli**[4], **Valerie Wells**[5], and **Daniel Zicha**[2]

[1]School of Biomedical and Health Sciences, King's College London, London SE1 9NH, UK

[2]Cancer Research UK London Resarch Institute, London WC2A 3LY, UK

[3]Department of Experimental Medicine, La Sapienza University, 00161 Rome, Italy

[4]Unit of General Pathology, Aging Research Center, G. D'Annunzio University Foundation, 66100 Chieti, Italy

[5]NYU in London, London WC1B 3RA, UK

Abstract

Activating mutations in Kras are the most frequent mutations in human cancer. They define a subset of patients who do not respond to current therapies and for whom prognosis is poor. Oncogenic Kras has been shown to deregulate numerous signalling pathways of which the most intensively studied are the Ras-ERK cascade and the PI3K-Akt cascade. However, to date there are no effective targeted therapies in the clinic against Kras-mutant cancers. Here we report that the βGBP cytokine, a physiological inhibitor of class I PI3Ks is a potent activator of apoptosis in Kras-mutant colorectal cancer cells, even when co-harboring mutant-activated PIK3CA. Our study unveils an elective route to intrinsic and extrinsic apoptosis which involves the cytoskeleton. Early events are inhibition of PI3K activity and Rac-independent actin rearrangement assignable to phosphoinositide changes at the plasma membrane. Cyclin E deregulation, arrest of DNA synthesis and Chk2 activation underscore events critical to the activation of an intrinsic apoptotic program. Clustering of CD95/Fas death receptors underscore events critical to the activation of extrinsic apoptosis. In nude mice we present the first evidence that xenograft tumor development is strongly inhibited by Hu-r-βGBP. Taken together our results open a new therapeutic opportunity against a subset of patients refractive to current treatments. This first demonstration of therapeutic efficacy against Kras-mutant colon cancer suggests that Hu-r-βGBP may also be therapeutically effective against other cancers harbouring activating Ras mutations as well as PIK3CA mutations.

Keywords

Kras; Rac; actin cytoskeleton; PI3K; Hu-r-βGBP; apoptosis

Corresponding Author: Livio Mallucci, School of Biomedical and Health Sciences, King's College London, Franklin Wilkins Building, 150 Stamford Street, London SE1 9NH, UK. Phone: +44 207 848 4257; Fax +44 207 848 4500; livio.mallucci@kcl.ac,uk.
*Current address: Department of Biochemistry and Molecular Biology, Shanghai Medical College of Fudan University, Shanghai 200032, P.R.China

Conflicts of interest: none

Europe PMC Funders Author Manuscripts

Introduction

Activating mutations in the Ras genes (H,K,N) (1), the most common oncogenic mutations in human cancers, are dominant determinants of drug resistance. Most frequent in Kras, Kras mutations define tumors refractory to conventional chemotherapy and radiation therapy (2, 3) and to more recently introduced therapies based on EGF receptor tyrosine kinase inhibitors (4-7). Locked in the GTP-bound mode, oncogenic Ras constitutively activates the Raf-MEK-ERK cascade and an integrated signaling network which controls cell proliferation and cell survival (8, 9) to be a major mediator of tumorigenesis.

The importance of activating mutations in the Ras oncogenes in human cancers has made Ras and downstream effectors elective targets for therapeutic intervention but the value of targeting inhibitors in the clinic remains doubtful. For example, prevention of Ras anchorage at the cell membrane by farnesyltransferase inhibitors has been shown to be effective in mice expressing oncogenic Ras but not in patients with solid tumors (10). Similarly, in more recent studies CI-1040, a MEK inhibitor, was found to induce significant shrinkage of Kras-driven lung carcinomas in mice (11) but to have no significant effect in patients with advanced lung, breast, colon and pancreatic cancers (12). Using a different approach a number of compounds with efficacy against cells with mutant-activated Kras have been identified by high-throughput screening (13-16) and shown to inhibit xenograft growth (13,15,16), however the mechanisms by which these compounds operate are not fully understood and their anti-cancer efficacy in the clinic remains uncertain.

Recently, the necessary role played by the PI3K/Akt pathway in maintaining tumor growth has made this pathway a target for small molecule inhibitors of the PI3K cascade (17-21). However, the efficacy of these inhibitors as single agents in Kras-driven oncogenesis is disputable. For example, in mice that had developed lung tumors in response to Kras activation, no significant tumor regression was found upon treatment with a dual pan-PI3K/mTOR inhibitor which had instead shown efficacy in lung tumors driven by the expression of activated PI3K (22). In other experiments, the efficacy of the PI3K inhibitor PX-866 was significantly less in xenografts bearing Kras and PIK3CA mutations than in those having PIK3CA mutations alone (23). On the other hand Kras-mutant lung tumors did regress when the pan-PI3K/mTOR inhibitor was used in combination with a MEK inhibitor (22). Similarly, in cells expressing Kras or Hras mutants, resistance to PI3K inhibitors could be reversed by inhibitors of the Ras-ERK pathway (24). Despite these positive results, it remains to be established whether in the human system Kras oncogenicity could be overcome by the combined targeting of the PI3K and the Ras pathways and be beneficial as, in addition to toxicity, a disadvantage of this approach is that these pathways are also required for the proliferation of normal cells and for the maintenance of their homeostatic balance.

In previous studies we have shown that monomeric β-galactoside binding protein (βGBP), an antiproliferative cytokine (25) which in normal cells participates in the negative regulation of the cell cycle (26) operates through mechanisms which involve high affinity receptor binding (Kd~1.5×10^{-10}M) (26) and molecular interactions leading to downregulation of class IA and class IB PI3Ks (27). Inhibition of PI3K activity by Hu-r-βGBP was found to have two major outcomes: suppression of Ras-GTP loading leading to block of ERK activation (27), and negation of akt gene expression leading to loss of Akt (21), conditions that either by blocking the ability of cancer cells to proliferate or by impairing their ability to survive can block oncogenicity, thus highlighting a selective anti-cancer effect as in normal cells βGBP enforced cell cycle restriction is reversible (26).

We now report that in colorectal carcinoma cells bearing oncogenic Kras downregulation of PI3K activity by Hu-r-βGBP at doses that did not inhibit canonical signaling downstream of Ras or PI3K promoted events critical to the activation of an intrinsic and an extrinsic cell death program initiating with Rac-independent actin reorganization assignable to phosphoinositide changes at the plasma membrane. We also report that Hu-r-βGBP had therapeutic efficacy in vivo and that the added presence of activating mutations in PIK3CA did not confer resistance to treatment with Hu-r-βGBP.

Materials and Methods

Cells

SW480, SW620 and LoVo cells were acquired from the American Type Culture Collection and cultured in Leibovitz's L-15 Medium with 10% fetal bovine serum. HCT116wt, HCT116mut, DLD1wt and DLD1mut cells, a gift from Bert Vogelstein (John Hopkins University) were cultured as originally reported (28). All cell lines were authenticated. Cell population distribution was assessed by propidium iodide staining and FACS analysis as reported previously (26). Epithelial cells of the normal colon mucosa from surgical interventions were obtained with informed consent and the study approved by the Medical School's Ethics Committee.

Recombinant βGBP

Hu-r-βGBP was expressed in *Escherischia coli* BL21(DE3) using hGal-1 cDNA in PET21a, purified by lactose-agarose (Sigma) affinity chromatography and purity assessed by MALDI-TOF.

Apoptosis assays

Tetramethylrhodamine ethyl ester (TMRE) (Molecular Probes/Invitrogen) staining, Annexin V (Pharmingen) staining and caspase-3 activity (OncoImmunin) were assessed according to manufacturers' instructions and analysed using an LSRII (Becton Dickinson).

PI3K assay

Step by step description of the method for assessment of PI3K activity has been reported previously (21). In brief, the immmunoprecipitated class I enzyme complex (27) was incubated in a kinase reaction for 3 hours with 40pmol phosphatidylinositol (4,5) biphosphate substrate and the phosphatidylinositol (3,4,5) triphosphate generated assayed in a competitive ELISA (Echelon Biosciences). Differences were tested using Student's t test and p-value < 0.05 was considered statistically significant.

Western blotting

ERK2 phosphorylation was visualized by mobility shift using anti-p42 polyclonal anitibodies (Santa Cruz Biotechnology). Phosphorylated Akt was detected by anti-phospho-Akt (Ser473) antibody (Cell Signaling Technology) and total Akt1/2 protein probed with anti-Akt1/2 antibodies (Santa Cruz Biotechnology). E2F1 was detected using anti-E2F1 polyclonal antibodies (Santa Cruz Biotechnology) and phosphorylated Chk2 detected with anti-phospho-Chk2 (Thr 68) polyclonal antibodies (Cell Signaling Technology). Secondary antibodies conjugated to horseradish peroxidase (GE Healthcare) were used for visualisation by enhanced chemiluminescence (GE Healthcare). Blots were reprobed with anti-GAPDH antibodies (Santa Cruz Biotechnology) or with monoclonal anti-β–actin (Sigma). Active Rac1 levels were assessed by affinity precipitation using PAK1 p21 binding domain agarose (Millipore) according to the manufacturer's instructions, followed by immunoblot analysis

using anti-Rac1 monoclonal antibody (Cell Signaling) and Odyssey fluorescent secondary antibodies. Total Rac was assessed using the same antibodies.

Fluorimetric quantitation of cyclin E

Cells fixed in cold 70% ethanol were treated with FITC-labelled monoclonal anti-cyclin E antibody (Becton Dickinson), washed, stained with propidium iodide containing RNase (Sigma) and analysed using an LSRII (Becton Dickinson). FITC fluorescence was collected using a 530/30 filter and propidium iodide fluorescencece using a 610/20 filter. At least 20,000 events were recorded.

DNA synthesis

Cells incubated with bromodeoxyuridine (BrdU) (Sigma) for 30 minutes were fixed in cold 70% ethanol and stained for BrdU uptake using a monoclonal anti-BrdU antibody (Becton Dickinson), followed by an FITC-labelled monoclonal goat anti-mouse antibody (Dako). DNA was counterstained with propidium iodide (Sigma) containing RNase (Sigma). Samples were analysed using an LSRII (Becton Dickinson) and FITC fluorescence collected using a 530/30 filter and propidium iodide fluorescence using a 610/20 filter. At least 20,000 events were recorded.

Microscopy

Cells on coverslips fixed in 3% paraformaldehyde/0.2%gluteraldehyde solution were stained with Texas Red phalloidin (Molecular Probes) for F-actin detection. For tubulin detection cells were treated with a monoclonal anti α-tubulin antibody (Sigma) followed by anti-mouse secondary antibody labeled with Alexa Fluor 488 (Molecular Probes). DNA was stained with DAPI (Sigma). Imaging was carried out using a Zeiss LSM 510 confocal system. Analysis of the F-actin labeled regions was performed in an automated manner using journals in MetaMorph software (Universal Imaging) and statistical significance tested by ANOVA (29). For CD95/Fas and FasL imaging with a Zeiss Axiophot microcope, cells were fixed in 4% paraformaldehyde, incubated with a monoclonal antibody to CD95/Fas (Abcam) followed by FITC-conjugated goat-anti-mouse IgG (Cappel) and rabbit polyclonal FasL antibody (Santa Cruz Biotechnology) followed by Texas Red-conjugated goat anti rabbit IgG (Jackson Immunoresearch Laboratories). Time-lapse imaging by Differential Interference Contrast microscopy was used to monitor peripheral dynamics at the plasma membrane edge. Recordings on sets of 150 cells from three randomly selected fields from double experiments were analysed and graded on a 0 to 3 arbitrary scale by two independent observers and statistical significance determined by χ^2 test.

Tumor growth in mice

Thymectomized female nude CD-1mice (Charles River Laboratory) were implanted subcutaneously in the right flank with 5×10^6 SW620 cells in 150 μl PBS. Control mice received an equal volume of PBS. Mice were ear marked and randomised in groups of seven and treatment with Hu-r-βGBP dissolved in PBS started at a tumor volume of ~40 mm^3. Treatment was performed by subcutaneous injection of 150μl in the tumor area for six consecutive days with one day interval, up to 35 days. Control mice received an equal volume of PBS. Experiments were carried out in accordance with the UK Coordinating Committee on Cancer Research guidelines and approved by the local responsible authorities.

Results

Arrest of cell replication and apoptosis are preceded by cytoskeletal rearrangement

We tested Hu-r-βGBP against SW480 and SW620 colorectal cancer cells, of primary and metastatic derivation, both harboring $Kras^{G12V}$ and against LoVo cells, also of metastatic origin, which harbor $Kras^{G13D}$ (COSMIC database). We found that treatment with Hu-r-βGBP at concentrations of 2-4 nM, some tenfold lower than those required for other cancer cells (21, 30) resulted in growth arrest and accumulation of cells in S phase, a state reversible in normal cells (26) but followed in the cells of this study by total cell loss attributable to the activation of an apoptotic program documented by changes in mitochondrial membrane potential, functional alteration of the plasma membrane and caspase 3 activation (Fig. 1A and 1B).

We next investigated whether as in other cell contexts (21, 27) PI3K was a responder to the action of Hu-r-βGBP. As cell phosphoinositide levels do not directly represent the functional state of the PI3K enzymes, but are the result of PI3K and PTEN activity, to estimate PI3K activity we isolated the PI3K enzyme complex (27) by immunoprecipitation and assessed its ability to convert phosphatidylinositol (4,5) biphosphate (PIP2) into phosphatidylinositol (3,4,5) triphosphate (PIP3) in a kinase reaction by measuring the generated PIP3 in a competitive ELISA (21). PIP3 quantitation (Fig. 2A) shows that downregulation of PI3K activity was a prime event, though delayed in the LoVo cells. However, contrary to previous evidence from other cell types (21, 27) we found no indication, after PI3K inhibition, of loss of ERK or Akt function whose phosphorylation state in the cells programmed to death was instead increased (Fig. 2B), a response conceivably similar to that seen in human cancer cells where inhibition of mTORC1 by a rapamycin derivative resulted in increase ERK and Akt activity via a feedback loop (31). We discovered instead that the treated cells had undergone a profound change of shape characterized by F-actin rearrangement, spreading of the microtubular network and an enlargement of the cell spread area whose changes in time were quantitated in terms of F-actin spatial distribution (Fig. 2C and 2D), changes that can block cancer cell motility and invasion (32) but in our case followed by apoptosis (Fig. 1B).

To investigate whether actin remodeling related to changes in Rac activity, a key regulator of actin dynamics, we assessed active Rac1 levels by immunoblot analysis and examined protrusive activity at the membrane edge, a Rac mediated process (33), by time-lapse imaging within the 24 hours time span leading to cytoskeletal changes. We found that in the cells where PI3K activity had been inhibited, Rac1 levels remained unchanged and edge membrane activity was not affected by treatment with Hu-r-βGBP, nor by treatment with wortmannin (10μM) a pharmacological p110 inhibitor. These results, consistent with the finding that edge ruffling induced by constitutively active Rac is not blocked upon PI3K inhibition (34), suggest that in cells harboring oncogenic Ras, Rac activation is maintained through Ras mediated signaling in a PI3K independent manner (35).

Cyclin E stabilization and arrest of DNA synthesis results in Chk2 activation

To determine which biochemical events consequent to PI3K inhibition and cytoskeletal changes might play a part in cell cycle arrest and in the activation of an apoptotic program, we examined parameters involved in cell growth restriction. Following immunoblot analysis, which in the arrested cells revealed no changes in cyclin D1 but raised and persistent levels of cyclin E and a gradual, and expected, decline of cyclin A levels, we quantitated cyclin E by cytofluorometry and found that while decreasing in the replicating cells, in the arrested cells cyclin E levels remained ectopically high with resulting relative values greater than those of controls by about 60-90 percent at the highest point (Fig. 3A).

As ectopic expression of cyclin E can cause impairment of DNA replication due to defects in replication initiation (36), we investigated whether in the arrested cells DNA synthesis had been inhibited. We found that by day 2 of treatment DNA synthesis had come to a halt (Fig. 3B). Since processes that interfere with DNA synthesis may result in the activation of DNA damage checkpoints and death by apoptosis (37), we turned our attention to the downstream kinase effectors of the DNA damage response pathways (37-39). Checkpoint kinase 1 (Chk1) was not detectable but we found that checkpoint kinase 2 (Chk2) which is required for responses to DNA damage and replication block (37, 39) had been activated (Fig. 3C). This is of relevance as Chk2 can phosphorylate E2F-1 regulating its stability and transcriptional activity (38, 40) and be a cause of apoptotic induction in cells where, in contrast to normal cells, E2F-1 is overexpressed (41, 42), as can be seen when comparing epithelial cells from the normal colon mucosa and the colon cancer cells of this investigation (Fig. 3 D and 3E).

Involvement of death receptors

Further to the rearrangement of cytoskeletal architecture (Fig. 2B) it is conceivable that rearrangement in the organization of subcortical actin may affect macromolecular mobility within the plane of the plasma membrane. We therefore investigated whether treatment with Hu-r-βGBP would affect the distribution pattern of the CD95/Fas death receptor which, as well as other death receptors (28), is a mediator of apoptosis, and examined whether the distribution pattern of Fas L would change accordingly. The evidence collected (Fig. 4) shows that as suggested by their co-location, CD95/Fas-Fas L clustering, a prime condition for the activation of an extrinsic apoptotic program, was detectable in each cell line.

Hu-r-βGBP has efficacy in vivo

Next we tested whether the therapeutic efficacy observed in vitro could be reproduced in an in vivo model. We implanted subcutaneously SW620 metastatic cells in nude mice and initiated treatment at a tumor volume of ~40 mm^3 administering Hu-r-βGBP at doses conforming to the nM dosages (Fig. 5 legend) used in the current and in previous in vitro experiments (21, 27, 30). Comparison of growth curves (Fig. 5A) shows that a five week period of treatment had inhibited xenograft growth by ~70%, with none of the treated mice appearing unhealthy as assessed by observation of behaviour and body weight measurements.

On further observation once the treatment had been stopped, we followed individually surviving mice bearing small tumors (~100-200mm^3) (Fig. 5B) and compared the rate of tumor growth resumption with the growth rate of control xenografts from an average volume of ~100 mm^3 hence. Histograms show that resumption of tumor development proceeded at a slower rate and that in only two instances within a nine week period xenograft size had approached the size attained in three weeks by the xenografts of the control mice (Fig. 5C).

Mutant PIK3CA does not confer resistance to Hu-r-βGBP

In addition to oncogenic Kras, whose frequency in human colorectal cancer is about 40%, activating mutations in the PIK3CA gene, also frequent in colorectal cancer (43), can induce oncogenicity (44) and tumor invasion (45). To investigate whether Hu-r-βGBP would be therapeutically effective in colorectal cancer cells bearing both mutations we examined HCT116 and DLD1 both mutated at Kras-G13D (13) in which either the mutant or the wild-type PIK3CA allele had been deleted by homologous recombination in order to express one of two major hot spot mutations (44). In a tightly controlled experiment we examined $HCT116^{G13D}$ cells harboring an H1047R alteration in exon 20 (kinase domain) and $DLD1^{G13D}$ cells which have an E545K alteration in exon 9 (helical domain) paired with their isogenic wild-type counterparts. Our results show that compared to the wild type the

growth rate of cells harboring mutant PIK3CA was increased and apoptosis was delayed by one day (DLD1mut) (Fig. 6A and 6B), but the response to Hu-r-βGBP was fundamentally similar in all cells whether PIK3CA wild type or mutant and similar to the response of the colorectal carcinoma cells of Figure 1 which are exempt of PIK3CA mutations. Inhibition of PI3K activity was followed by inhibition of cell proliferation and cell death assignable to the activation of an apoptotic program.

Discussion

Mutant-activated Kras defines a subset of patients with poor prognosis. We show that the PI3K inhibitor used in this study was remarkably efficacious. Hu-r-βGBP as a single agent induced apoptotic death in cancer cells harboring mutant-activated Kras, even when co-expressing an activating mutation in PIK3CA, and was therapeutically effective in vivo.

Unlike molecules designed to target critical hubs within signaling pathways, the βGBP molecule operates through mechanisms which involve high affinity receptor binding (26) and molecular interactions leading to functional inhibition of the p110 catalytic subunit of class IA and class IB PI3Ks with consequent loss of ERK (27) and Akt function (21). Surprisingly, in the cancer cells of this study inhibition of PI3K activity was not characterized by loss of active ERK or active Akt, key prognostic therapeutic markers to βGBP response (46), whose phosphorylation state was instead increased, but characterized by actin reorganization in a Rac-independent manner.

While our data provide no indication that changes in actin organization related to loss of Rac activity, the fact that phosphoinositides and PIP2 in particular have an important role in the binding and control of actin regulatory proteins (47) lends ground to infer that changes in PIP2 levels, turnover or spatial distribution brought about by molecular interactions involved in βGBP receptor-PI3K communication (27) may affect plasma membrane-cytoskeletal linkages and have a causative role in the activation of two distinct sets of events critical to the initiation of an apoptotic program. One, relating to a general rearrangement of the cytoskeleton, consequent cell cycle checkpoint restrictions and the ectopic accumulation of cyclin E whose bearing on the impairment of DNA replication provides a potential for errors in DNA repair and for the activation of an intrinsic apoptotic process. The other set of events relates, conceivably, to changes in cortical actin organization, increased macromolecular mobility within the plane of the plasma membrane and clustering of death receptors, a critical condition for the activation of an extrinsic apoptotic process.

Two other aspects of our study deserve mention. One pertains to the importance that activating mutations in the PIK3CA gene have in conferring advantages which facilitate cell growth and invasion (44). Our data (Fig. 6) provide strong evidence that in colorectal carcinoma cells harboring mutated PIK3CA further to oncogenic Kras, inhibition of PI3K activity was followed by the activation of a cell death program, underscoring that as single agent Hu-r-βGBP had full therapeutic efficacy where combination targeting of PI3K and of Ras downstream effectors might instead be required (22, 24). The other key aspect relates to the ability of Hu-r-βGBP to strongly reduce tumor growth and to convert tumors that had survived a five week period of treatment from a faster to a slow developing (Fig. 5B and 5C) and, conceivably, a more benign tumor phenotype. Based on a model discussed in a previous report (21) this result may be interpreted as proof-of-principle-evidence that cancer vulnerability in response to Hu-r-βGBP challenge is greater in the aggressive cancer phenotype, as a contained tumor growth after end of treatment is suggestion of clonal selection through elimination of the more aggressive cells.

Recently, a number of compounds identified by high-throughput screening have been reported to have therapeutic efficacy against Kras-mutant cancer cells (13-16), however, amongst all candidate agents for the therapy of cancers harboring mutant-activated Ras, the βGBP molecule, a cytokine, by virtue of its physiological nature is the only one, to our knowledge, which in the clinic would be implicitly exempt from drug toxicity and drug resistance. As, further to colorectal carcinoma, mutations in the Ras oncogenes and in genes involved in PI3K regulation extend to other cancers, our results suggest that Hu-r-βGBP is, potentially, a therapeutic agent that could provide benefit to a large number of patients.

Acknowledgments

PI3-Kinase ELISA Kits were generously provided by Echelon Biosciences. We are indebted to Bert Vogelstein (John Hopkins University) for generously providing cell lines HCT116 wt/null, HCT116 mut/null, DLD1 wt/null and DLD1 mut/null. We are grateful to Julian Downward and to Esther Castellano for advice and expertise concerning Rac assessment. We thank Cosmo Rossi for management of xenograft study and Simone Martino for technical assistance. We are grateful to Roger Morris for his support, to Paul Nielsen for his interest and to Giampietro Schiavo for critical reading of the manuscript. We acknowledge with gratitude the art work and kindness of the late Kate Kirwan.

Grant support This work was supported by a KCL/Peoples Republic of China KC Wong fellowship award (D. Shi), by two MIUR grants (L. Lotti and R. Mariani-Costantini), by AIRC grant # IG 9168 (R. Mariani-Costantini) and by funding from Cancer Research UK (D. Davies, P. Jordan, A. Nicol and D. Zicha).

References

1. Barbacid M. Ras genes. Annu Rev Biochem. 1987; 56:779–827. [PubMed: 3304147]
2. Cengel KA, Voong KR, Chandrasekaran S, Maggiorella L, Bruner S, Stanbridge S, et al. Oncogenic K-Ras signals through epidermal growth factor receptor and wild-type H-Ras to promote radiation survival in pancreatic and colorectal carcinoma cells. Neoplasia. 2007; 9:341–348. [PubMed: 17460778]
3. Mascaux C, Iannino N, Martin B, Paesmans M, Berghmans T, Dusart M, et al. The role of RAS oncogene in survival of patients with lung cancer. A systematic review of the literature with meta-analysis. Br J Cancer. 2005; 92:131–139. [PubMed: 15597105]
4. Pao W, Wang T, Riely GJ, Muiller VA, Pau Q, Ladanyi M, et al. KRAS mutations and primary resistance of lung adenocarcinomas to gefitinib or erlotinib. PLoS Med. 2005; 2:e17. [PubMed: 15696205]
5. Massarelli E, Varella-Garcia M, Tang X, Xavier AC, Ozburn NC, Liu DD, et al. KRAS mutation is an important predictor of resistance to therapy with epidermal growth factor receptor tyrosine kinase inhibitors in non-small-cell lung cancer. Clin Cancer Res. 2007; 13:2890–2896. [PubMed: 17504988]
6. Jhawer M, Goel S, Wilson AJ, Montagna C, Ling Y-H, Byun D-S, et al. PIK3CA mutation/PTEN expression status predicts response of colon cancer cells to the epidermal growth factor receptor inhibitor cetuximab. Cancer Res. 2008; 68:1953–1961. [PubMed: 18339877]
7. Van Cutsem E, Kohne C-H, Hitre E, Zaluski J, Chine C-RC, Makhson A, et al. Cetuximab and chemotherapy as initial treatment for metastatic colorectal cancer. New Engl J Med. 2009; 360:1408–1417. [PubMed: 19339720]
8. Downward J. Targeting Ras signaling pathways in cancer therapy. Nat Rev Cancer. 2003; 3:11–22. [PubMed: 12509763]
9. Gupta S, Ramjaun AR, Haiko P, Wang Y, Warne PH, Nicke B, et al. Binding of Ras to phosphoinositide 3-kinase p110α is required for Ras-driven tumorigenesis in mice. Cell. 2007; 129:957–968. [PubMed: 17540175]
10. Kohl NE, Omer CA, Conner MW, Anthony NJ, Davide JP, Desolms SJ, et al. Inhibition of farnesyltransferase induces regression of mammary and salivary carcinomas in ras transgenic mice. Nat Med. 1995; 1:792–797. [PubMed: 7585182]

11. Ji H, Wang Z, Pereira S, Li D, Liang M-C, Zaghlul S, et al. Mutations in BRAF and KRAS converge on activation of the mitogen-activated protein kinase pathway in lung cancer mouse models. Cancer Res. 2007; 67:4933–4939. [PubMed: 17510423]
12. Rinehart J, Adjei AA, LoRusso PM, Waterhouse D, Hecht JR, Natale RB, et al. Multicellular phase II study of the oral MEK inhibitor, C1040, in patients with advanced non-small-cell lung, breast, colon, and pancreatic cancer. J Clin Oncol. 2004; 22:4456–4462. [PubMed: 15483017]
13. Torrance CJ, Agrawal V, Vogelstein B, Kinzler KW. Use of isogenic human cancer cells for high-throughput screening and drug discovery. Nature Biotech. 2001; 19:940–945.
14. Dolma S, Lessnick SL, Hahn WC, Stockwell BR. Identification of genotype-selective antitumor agents using synthetic lethal chemical screening in engineered human tumor cells. Cancer Cell. 2003; 3:285–296. [PubMed: 12676586]
15. Guo W, Wu S, Liu J, Fang B. Identification of a small molecule with synthetic lethality for K-Ras and protein kinase C iota. Cancer Res. 2008; 68:7403–7408. [PubMed: 18794128]
16. Shaw AT, Winslow MM, Magendantz M, Ouyang C, Dowdle J, Subramanian A, et al. Selective killing of K-ras mutant cancer cells by small molecule inducers of oxidative stress. Proc Natl Acad Sci USA. 2011; 108:8773–8778. [PubMed: 21555567]
17. Hennessy BT, Smith DL, Ram PT, Lu Y, Mills GB. Exploiting the PI3K/Akt pathway for drug discovery. Nat Rev Drug Discov. 2000; 4:988–1004. [PubMed: 16341064]
18. Vivanco I, Sawyers CL. The phosphatidylinositol 3-kinase-Akt pathway in human cancer. Nat Rev Cancer. 2002; 2:489–501. [PubMed: 12094235]
19. Lim KH, Counter CM. Reduction in the requirement of oncogenic Ras signaling to activation of PI3K/AKT pathway during tumor maintenance. Cancer Cell. 2005; 8:381–392. [PubMed: 16286246]
20. Shaw R, Cantley LC. Ras, PI(3)K and mTOR signaling controls tumour cell growth. Nature. 2006; 441:424–430. [PubMed: 16724053]
21. Wells V, Mallucci L. Phosphoinositide 3-kinase targeting by the β galactoside binding protein cytokine negates akt gene expression and leads aggressive breast cancer cells to apoptotic death. Breast Cancer Res. 2009; 11:R2, 1–10. [PubMed: 19133120]
22. Engelman JA, Chen L, Tan X, Crosby K, Guimaraes AR, Upadhyay R, et al. Effective use of PI3K and MEK inhibitors to treat mutant *Kras* G12D and *PIK3CA* H1047R murine lung cancers. Nat Med. 2008; 14:1351–1356. [PubMed: 19029981]
23. Ihle NT, Lemos R Jr, Wipf P, Yacoub A, Mitchell C, Siwak D, et al. Mutations in the phosphatidylinositol-3-kinase pathway predict for antitumor activity of the inhibitor PX-866 whereas oncogenic Ras is a dominant predictor for resistance. Cancer Res. 2009; 69:143–150. [PubMed: 19117997]
24. Torbett NE, Luna-Moran A, Knight ZA, Houk A, Moasser M, Weiss W, et al. A chemical screen in diverse breast cancer cell lines reveals genetic enhancers and suppressors of sensitivity to PI3K isoform-selective inhibition. Biochem J. 2008; 415:97–110. [PubMed: 18498248]
25. Blaser C, Kaufman M, Muller C, Zimmerman C, Wells V, Mallucci L, et al. β-galactoside binding protein secreted by activated T cells inhibits antigen-induced proliferation of T cells. Eur J Immunol. 1998; 28:2311–2319. [PubMed: 9710209]
26. Wells V, Mallucci L. Identification of an autocrine negative growth factor: mouse-β-galactoside binding protein is a cytostatic factor and cell growth regulator. Cell. 1991; 64:91–97. [PubMed: 1986871]
27. Wells V, Downward J, Mallucci L. Functional inhibition of PI3K by the βGBP molecule suppresses Ras-MAPK signaling to block cell proliferation. Oncogene. 2007; 26:7709–7714. [PubMed: 17603562]
28. Cummins JM, Kohli M, Rago C, Kinsler KW, Vogelstein B, Bunz F. X-linked inhibitor of apoptosis protein (XIAP) is a nonredundant modulator of tumor necrosis factor-related apoptosis-inducing ligand (TRAIL)-mediated apoptosis in human cancer cells. Cancer Res. 2004; 64:3006–3008. [PubMed: 15126334]
29. Zicha D, Genot E, Dunn GA, Kramer IJM. TGFβ1 induces a cell cycle-dependent increase in motility of epithelial cells. J Cell Sci. 1999; 112:447–454. [PubMed: 9914157]

30. Ravatn R, Wells V, Nelson L, Vettori D, Mallucci L, Chin KV. Circumventing multidrug resistance in cancer by β-galactoside binding protein, an antiproliferative cytokine. Cancer Res. 2005; 65:1631–1634. [PubMed: 15753355]
31. Carracedo A, Ma L, Teruya-Felstein J, Roojo F, Salmena L, Alimonti A, et al. Inhibition of mTORC1 leads to MAPK pathway activation through a PI3K-dependent feedback loop in human cancer. J Clin Invest. 2008; 118:3065–3074. [PubMed: 18725988]
32. Rosenthal DT, Iyer H, Escudero S, Bao L, Wu Z, Ventura AC, et al. p38γ promotes breast cancer cell motility and metastasis through regulation of RhoC GTPase, cytoskeletal architecture, and anovel leading edge behaviour. Cancer Res. 2011; 71:6338–6349. [PubMed: 21862636]
33. Burridge K, Wennerberg K. Rho and Rac take center stage. Cell. 2004; 116:167–179. [PubMed: 14744429]
34. Nobes D, Hawkins P, Stephens L, Hall A. Activation of the small GTP-binding proteins rho and rac by growth factor receptors. J Cell Sci. 1995; 108:225–233. [PubMed: 7738099]
35. Lambert M, Lambert QT, Reuther GW, Malliri A, Siderovski DP, Sondek J, et al. Tiam1 mediates Ras activation of Rac by a PI(3)K-independent mechanism. Nat Cell Biol. 2002; 4:621–625. [PubMed: 12134164]
36. Ekholm-Reed S, Mendez J, Tedeco D, Zetterberg A, Stillman B, Reed SI. Deregulation of cyclin E in human cells interferes with prereplication complex assembly. J Cell Biol. 2004; 165:789–800. [PubMed: 15197178]
37. Zhou BB, Elledge SJ. The DNA damage response: Putting checkpoints in perspective. Nature. 2000; 408:433–439. [PubMed: 11100718]
38. Lin WC, Lin FT, Nevins JR. Selective induction of E2F1 in response to DNA damage mediated by ATM-dependent phosphorylation. Genes Dev. 2001; 15:1833–1844. [PubMed: 11459832]
39. Kastan MB, Bartek J. Cell cycle checkpoints and cancer. Nature. 2004; 432:316–323. [PubMed: 15549093]
40. Stevens C, Smith L, La Thangue NB. Chk2 activates E2F-1 in response to DNA damage. Nat Cell Biol. 2003; 5:401–409. [PubMed: 12717439]
41. Krek W, Xu G, Livingston D. Cyclin A-kinase regulation of E2F-1 DNA binding function underlies suppression of an S phase checkpoint. Cell. 1995; 83:1149–1158. [PubMed: 8548802]
42. Fueyo J, Gomez-Manzano C, Jung WK, Liu TJ, Alemany R, McDonnell TJ, et al. Overexpression of E2F-1 in glioma triggers apoptosis and suppresses tumor growth in vitro and in vivo. Nat Med. 1998; 4:685–690. [PubMed: 9623977]
43. Samuels Y, Wang Z, Bardelli A, Silliman N, Ptak J, Szabo S, et al. High frequency of mutations of the PIK3CA gene in human cancers. Science. 2004; 304:554. [PubMed: 15016963]
44. Bader AG, Kang S, Vogt P. Cancer specific mutations in PIK3CA are oncogenic in vivo. Proc Natl Acad Sci USA. 2006; 103:1475–1479. [PubMed: 16432179]
45. Samuels Y, Diaz L Jr, Schmidt-Kittler O, Cummins JM, Delong L, Cheong I, et al. Mutant PIK3CA promotes cell growth and invasion of human cancer cells. Cancer Cell. 2005; 7:561–573. [PubMed: 15950905]
46. Mallucci, L.; Wells, V. βGBP, compositions comprising βGBP, and related methods and uses thereof. US Patent. 7,994,113. 2011.
47. Di Paolo G, De Camilli P. Phosphoinositides in cell regulation and membrane dynamics. Nature. 2006; 443:651–657. 2006. [PubMed: 17035995]

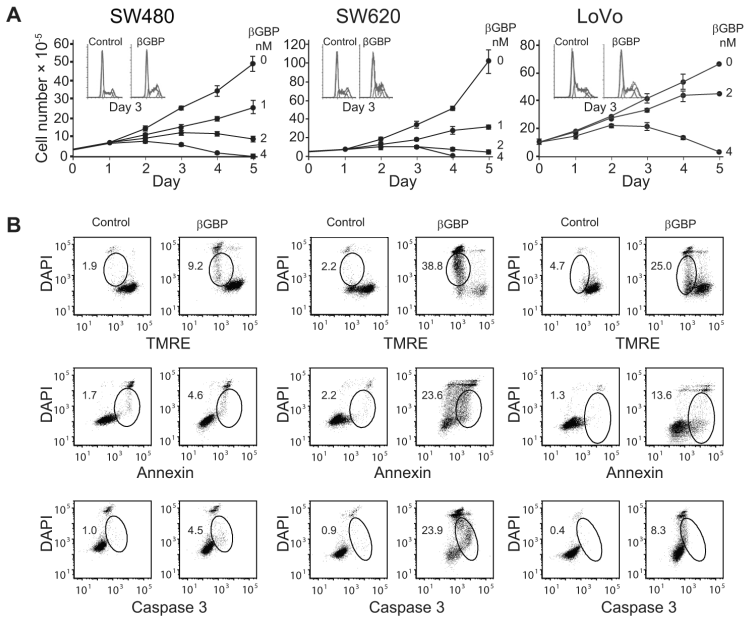

Figure 1.

Treatment with Hu-r-βGBP inhibits cell proliferation and induces apoptosis**.**

A, Rate of cell proliferation as related to dose response. Values are means of triplicate cultures +/− standard error of the mean (SEM). Insets show cell cycle phase distribution at day 3 of treatment with 4nM Hu-r-βGBP. Hu-r-βGBP added at hour 6 after seeding. B, Apoptotic events at day 3 of treatment. Top to bottom: mitochondrial membrane potential assessed by tetramethylrhodamine ester (TMRE) staining**;** phosphatidylserine orientation at the plasma membrane assessed by Annexin V staining; caspase-3 activity assessed using PhiPhiLux. Inset values are percentages of cells committed to apoptosis (encircled area). Hu-r-βGBP 4nM added at hour 6 after seeding. Data are from parallel representative experiments.

Europe PMC Funders Author Manuscripts

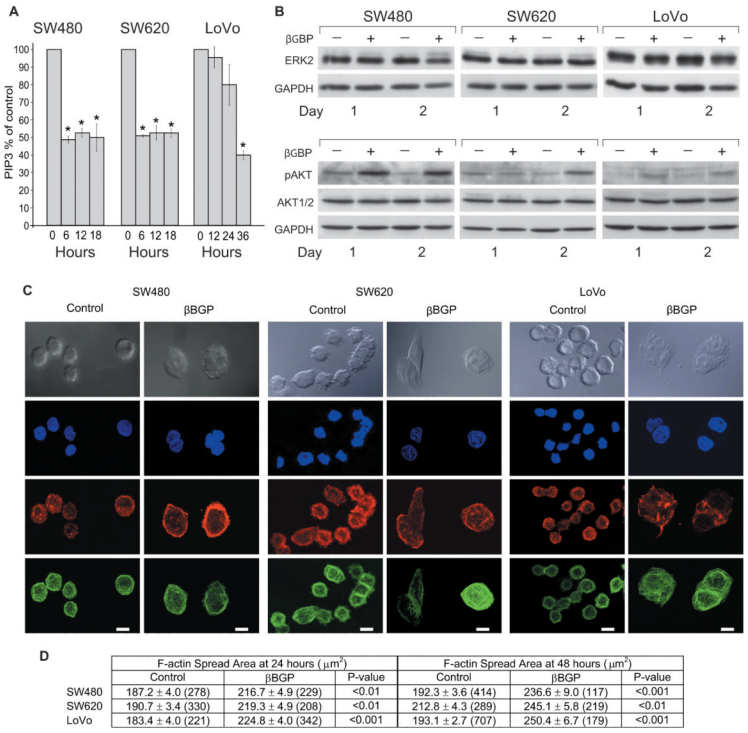

D

	F-actin Spread Area at 24 hours (μm²)			F-actin Spread Area at 48 hours (μm²)		
	Control	βBGP	P-value	Control	βBGP	P-value
SW480	187.2 ± 4.0 (278)	216.7 ± 4.9 (229)	<0.01	192.3 ± 3.6 (414)	236.6 ± 9.0 (117)	<0.001
SW620	190.7 ± 3.4 (330)	219.3 ± 4.9 (208)	<0.01	212.8 ± 4.3 (289)	245.1 ± 5.8 (219)	<0.01
LoVo	183.4 ± 4.0 (221)	224.8 ± 4.0 (342)	<0.001	193.1 ± 2.7 (707)	250.4 ± 6.7 (179)	<0.001

Figure 2.

Inhibition of PI3K activity is followed by changes of cell morphology brought about by cytoskeletal rearrangement. A, Assessment of PI3K activity as measurements of phosphatidylinositol (3,4,5)-triphosphate (PIP3) expressed as percentages of controls. Hu-r-βGBP 4nM added at hour 6 after seeding. Values are means of triplicate measurements +/− SEM. *$p < 0.05$ versus controls. B, Western blotting. Top panels: ERK2 mobility shift, upper band represents phosphorylated protein. Bottom panels: phosphorylated (Ser473) Akt and total Akt protein. GAPDH is shown as loading control. Hu-r-βGBP 4nM added at hour 6 after seeding. Data are from a representative experiment.

C, Example micrographs of control and treated cells. Gray images show cell morphology acquired using Differential Interference Contrast microscopy. Blue images represent nuclei labeled with DAPI; red images represent F-actin distribution; green images represent microtubules. Images acquired by laser scanning confocal microscopy. Hu-r-βGBP 4nM added at hour 6 after seeding. SW480 cells fixed at hour 24 of treatment, SW620 and LoVo cells fixed at hour 48. Scale bars 10μm. D, Quantitation of cell spread area as defined by F-actin staining. Values are means +/−SEM. Data acquired in automated manner in MetaMorph software and analysed by ANOVA (29) in Mathematica 4.2. Values in brackets represent the number of cells measured.

Europe PMC Funders Author Manuscripts

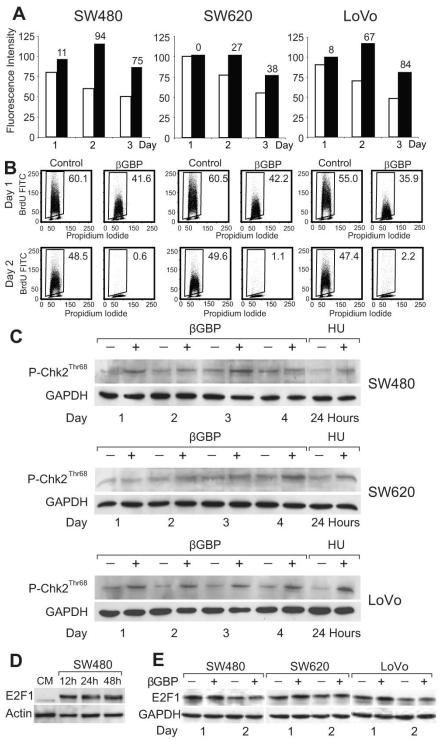

Figure 3.

Cyclin E stabilization and arrest of DNA synthesis result in Chk2 activation.

A, Assessment of cyclin E by cytofluorometry in untreated (white histograms) and treated cells (black histograms). Numbers on histograms represent percentage differences between control and treated cells. B, DNA synthesis assessed by BrdU uptake. Inset numbers represent percentage of cells positive for BrdU. C, Western blots of phosphorylated Chk2 in untreated and treated cells and in control cells treated with 1mM hydroxyurea (HU). GAPDH is shown as loading control.

D, Western blots representing constitutive E2F1 levels in epithelial cells from normal human colorectal mucosa (CM) and in SW480 cells. β-actin is shown as loading control. E, Western blots of E2F1 in untreated and treated cells. Slower migrating dense bands represent the phosphorylated protein. GAPDH is shown as loading control. Hu-r-βGBP 4nM added at hour 6 after seeding. Data are from single representative experiments.

Europe PMC Funders Author Manuscripts

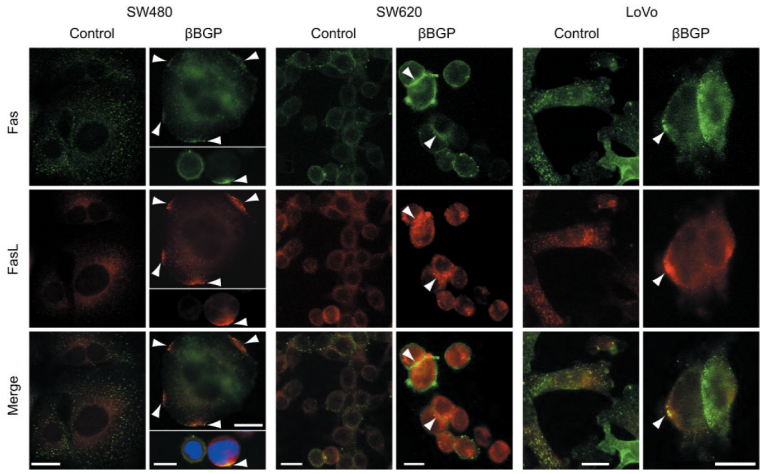

Figure 4.

Localization of CD95/Fas and FasL in controls and in treated cells. Control cells show punctuate staining for both CD95/Fas (green) and FasL (red) with low levels of co-localization (bottom, merge). Treated cells show clustering of CD95/Fas (green) and clustering of FasL (red) which can be frequently found at the same localisation on cell surfaces (bottom, merge). Examples of this clustering are indicated by arrow heads. Hu-r-βGBP 4nM added at hour 6 after seeding. SW480 cells fixed at hour 24 of treatment, SW620 and LoVo cells fixed at hour 48. Scale bars 10μm.

Europe PMC Funders Author Manuscripts

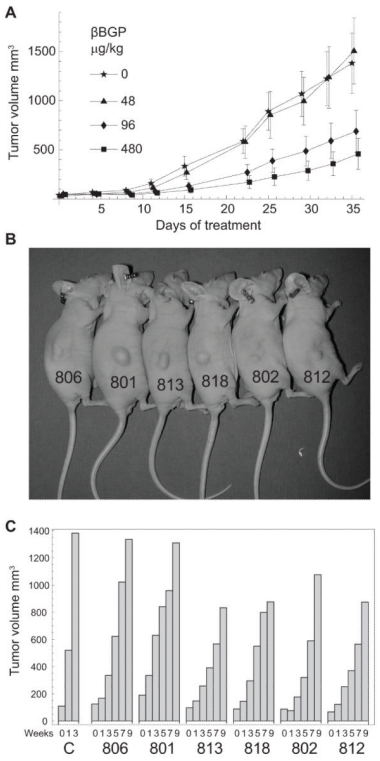

Figure 5.

Hu-r-βGBP inhibits tumor development in nude mice. A, Rate of SW620 cell xenograft growth as related to dose response. Values are means +/− SEM from groups of seven mice. Doses in μg/kg conform to the nM in vitro dosages used in the current experiments and in previous experiments (21, 30): 48μg/kg = 3.2nM; 96μg/kg = 6.4nM; 480μg/kg = 32nM. Calculation based on arbitrary animal weight to volume equivalence of 1:1. (1g =1ml). B, Individually marked mice bearing small tumors (~100-200mm^3 average size) at the end of a five week treatment. C, Rate of tumor development in untreated control mice [C] from an average xenograft size of ~100mm^3 and rate of resumption of growth in the mice of panel B after cessation of treatment**.**

Europe PMC Funders Author Manuscripts

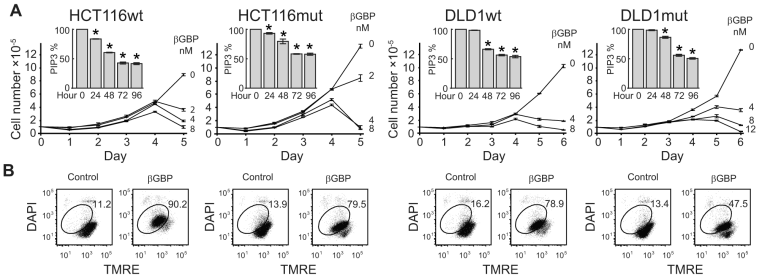

Figure 6.

Hu-r-βGBP overcomes Kras and PIK3CA mutations. A, Growth curves show rate of cell proliferation as related to dose response in PIK3CA wild type (wt) and in PIK3CA mutant (mut) colorectal cancer cells. Values are means of triplicate cultures +/− SEM. Inset histograms represent PI3K activity as measurements of phosphatidylinositol (3,4,5)-triphosphate (PIP3) expressed as percentages of controls. Values are means of triplicate measurements +/− SEM. *p < 0.05 versus controls. Hu-r-βGBP 8nM or 12nM (DLD1mut) added at hour 6 after seeding. B, Loss of mitochondrial membrane potential assessed by tetramethylrhodamine ester (TMRE) staining at day 4 or 5 (DLD1mut). Inset values are percentages of cells committed to apoptosis (encircled area). Hu-r-βGBP added at hour 6 after seeding.

Europe PMC Funders Author Manuscripts